



Diseases of the Sella Turcica and Parasellar Region

1

W. Kucharczyk and L. A. Loevner

Abstract

Knowledge of the anatomy in the regions of the sella turcica, suprasellar cistern, and cavernous sinus paired with clinical history and presentation is important for accurate image interpretation. Focused diagnosis of lesions in these regions requires identifying the anatomic location in which a lesion arises, evaluation of specific imaging findings inherent to the lesion as well as in the surrounding structures, and correlation with clinical presentation (symptoms and signs).

It is important to determine whether a mass arises in the sella turcica versus the suprasellar cistern, and whether it involves both the sella turcica and suprasellar cistern.

Imaging features of a sellar mass that should be assessed include:

- Arising from or separate from the pituitary gland
- Cystic degeneration
- Size of the sella
- Infundibulum involved
- Stalk deviation
- Relationship to chiasm
- Edema optic pathways, hypothalamus
- Cavernous sinus—internal carotid artery
- Osseous remodeling, destruction

Keywords

Pituitary gland · Pituitary stalk · Sella turcica · Suprasellar cistern · Magnetic resonance imaging · CT imaging · Pituitary adenomas

W. Kucharczyk (✉)
Department of Radiology, University of Toronto,
Toronto, ON, Canada
e-mail: w.kucharczyk@utoronto.ca

L. A. Loevner
Neuroradiology Division, Department of Radiology, University of
Pennsylvania, Philadelphia, PA, USA

Learning Objectives

- Review anatomy of the sella turcica and parasellar regions.
- Illustrate distinguishing imaging findings of the most common lesions arising from the sellar and parasellar regions.
- Use imaging findings in conjunction with clinical signs and symptoms to develop a concise differential diagnosis and the “single best” diagnosis.

Key Points

- Knowledge of the anatomy of the pituitary gland, pituitary stalk, cavernous sinus, suprasellar cistern, optic chiasm, and arteries of the central skull base is essential for accurate diagnosis.

1.1 Introduction

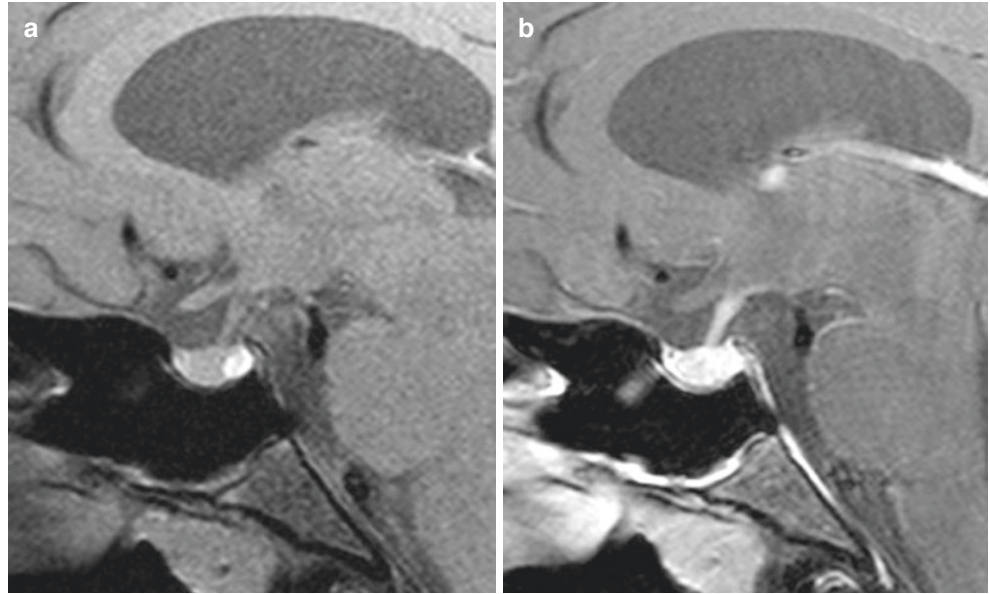
A spectrum of pathology affects the pituitary gland/sella turcica and the surrounding regions. The most common abnormality is a pituitary adenoma, followed by Rathke cleft cyst and meningioma. Magnetic resonance imaging (MRI) is the imaging modality of choice in the evaluation of sellar and parasellar pathology. Patients are referred for MRI most often on the basis of clinical and laboratory findings; however, it is also common to discover lesions in these regions as incidental findings on imaging of the brain performed for other indications. Computed tomography (CT) may be used to supplement MRI findings such as to evaluate for intra-lesional calcifications or changes in adjacent bones (remodeling, destruction, or hyperostosis).

1.2 Imaging Appearance of the Normal Pituitary Gland

The anterior lobe of the pituitary gland is isointense to brain on T1W and T2W imaging and demonstrates homogeneous

enhancement following contrast administration (Fig. 1.1a, b). The posterior lobe of the pituitary gland is often hyperintense on T1-weighted imaging and positioned slightly behind the adenohypophysis, often within a cup-shaped depression of the dorsum sellae (Fig. 1.1a).

Fig. 1.1 Normal pituitary gland unenhanced T1-weighted MR (a). Contrast-enhanced T1-weighted MR (b)



1.3 Pituitary Adenomas

The imaging work-up of pituitary adenomas remains largely unchanged over the last decade with the exception of the ability to more routinely perform high resolution sub-millimeter thin imaging in select cases where adenomas are often not detected on conventional sequences/techniques (Cushing's disease). Unenhanced and enhanced T1-weighted images are obtained in the sagittal and coronal planes as well as a T2-weighted sequence in the coronal plane. Dynamic contrast-enhanced T1-weighted imaging is also often acquired to evaluate for microadenomas. If the conventional MR imaging is negative or equivocal, and the patient has unequivocal symptoms and signs (lab work, etc.), additional imaging utilizing sub-millimeter sequences may be indicated.

Pituitary microadenomas (≤ 10 mm) are contained within the sella turcica and are often hypointense relative to the normal adenohypophysis on T1-weighted images. They are round in shape, and when over 5–6 mm in size often displaces the pituitary stalk away from the side of the lesion. Occasionally, pituitary adenomas may exhibit hyperintensity on T1-weighted images often reflecting internal hemorrhage. Such hemorrhage is more common in prolactinomas and may be spontaneous or following medicinal therapy such as bromocriptine. The signal intensity of microadenomas on T2W images varies, although if hyperintense relative to the normal gland, a microadenoma is likely. In the clinical and laboratory setting of excess growth hormone, a focal mass that is hypointense on T2-weighted images highly correlates with a diagnosis of a densely granulated GH-secreting adenoma. Following contrast administration, most pituitary adenomas show "differential enhancement" which means that they enhance but to a lesser degree than the normal surrounding avidly enhancing gland, so they appear relatively hypointense. Delayed contrast-enhanced imaging may inadvertently obscure microadenomas by virtue of their slower "wash-in" curve relative to normal pituitary. Dynamic contrast-enhancing imaging may be useful for some microadenomas, especially ACTH-secreting tumors.

Pituitary macroadenomas (defined as tumors greater than 10 mm in size) often extend beyond the confines of the sella, most often into the suprasellar cistern or the cavernous sinus. They may also grow inferiorly, invading the bone at the skull base and the sphenoid sinus. With trans-nasal endoscopic approaches being the mainstay in surgical management of sellar and parasellar pathology, the description of such extension is required in the preoperative imaging checklist.

Macroadenomas that grow superiorly into the suprasellar cistern are commonly bilobed "snowman" in shape, constrained at the waist by the diaphragma sella. Macroadenomas often are complex lesions with solid and cystic components resulting in heterogeneous signal on T1- and T2-weighted

imaging. Cystic and/or necrotic components (caused by poor tumoral blood supply) exhibit variable signal, but often contain proteinaceous debris which may be hyperintense on T1-weighted images, and hypo- to hyperintense on T2-weighted imaging depending on the protein concentration. With macroadenomas, the neurohypophysis/stalk may be compressed, laterally displaced, or difficult to visualize. In some cases, compression of the infundibulum is disruptive such that the neurohypophyseal function is displaced upstream with a "new" bright spot more cephalad along the infundibulum.

Cavernous sinus involvement may be due to compressive growth and consequent medial and occasionally lateral dural reflection or may reflect true invasion of the sinus. Invasion is excluded if normal pituitary tissue is seen between the tumor and the sinus. On imaging, cavernous invasion is suggested when neoplasm is present lateral to the cavernous internal carotid artery (Knosp criteria grade 3A, 3B, and 4).

While prolactinomas and growth hormone (GH)-secreting adenomas are often located laterally in the sella turcica, ACTH-secreting adenomas in Cushing's disease are usually quite small in size, more difficult to detect, and are more often located in the midline. Because of the morbidity associated with this disease, ACTH-secreting lesions require the most detailed and exhaustive imaging with the intent to provide surgical management.

GH-secreting adenomas have the unique characteristic of exhibiting hypointensity on T2-weighted images in two-thirds of cases, usually the densely granulated subtype. Spontaneous infarction or necrosis of GH-secreting adenomas is not uncommon. Some cases of acromegaly detected late in the course of the disease exhibited an enlarged, partially empty sella turcica, lined with adenomatous tissue that proved difficult to analyze. Medical treatment based on octreotide analogs (somatostatin) decreases the size of the adenoma on average by 35% and brings the level of somatomedin C back to normal in 50% of cases.

Hemorrhage occurs in 20% of all pituitary adenomas, but it is usually occult. Pituitary apoplexy with severe headache, cranial nerve palsy, and significant hypopituitarism is generally caused by marked hemorrhage within a macroadenoma.

Surgery of the sella and parasellar region is usually undertaken via an endonasal transsphenoidal endoscopic approach for a number of reasons. Multiple instruments can be utilized including angled endoscopes. A nasoseptal flap can be harvested at the time of surgery to reconstruct the skull base and thus prevent CSF leaks. Furthermore, the exposure can be lateralized to resect parasellar lesions and can be extended posteriorly through the clivus to reach the prepontine cistern. Preoperative CT is routinely performed for intraoperative surgical navigation. CT also reveals bony anatomy including the location of sphenoidal sinus septae and their insertions,

the presence of onodi cells, and the degree of aeration of the sphenoid sinus, all of which may influence the surgical approach, patient safety, and ultimately patient outcome.

1.4 Postoperative Sella Turcica

The surgical cavity immediately after endonasal transsphenoidal surgery is often filled with packing material. Surgicel is frequently used and is impregnated with blood and secretions. The presence of packing material, secretions, and adhesions usually keeps the surgical cavity from collapsing in the days and weeks following surgery. Blood, secretions, and packing material slowly involute over the following 2–3 months. Even after a few months, fragments of blood-impregnated surgicel can still be found in the surgical cavity. If the diaphragm is disrupted during surgery, fat or muscle implants are inserted by the surgeon to prevent the development of a cerebrospinal fluid fistula. Their resorption takes much longer. Implanted fat involutes slowly and may exhibit hyperintensity on the T1-weighted image up to 2–3 years after surgery. An MRI study performed 48 h after surgery checks for potential complications and may visualize what appears to be residual tumor, i.e., a mass of intensity identical to that of the adenoma before surgery that commonly occupies a peripheral portion of the adenoma. This early investigation is extremely helpful to interpret the follow-up MR examinations. Magnetic resonance imaging 2–3 months after surgery is essential to check for residual tumor. Subsequent surveillance MRIs, 1–2 years or more following surgical resection, may illustrate a progressively enlarging mass indicative of recurrent adenoma.

Key Points

- The most common lesions in the sella turcica are pituitary adenomas (microadenomas > macroadenomas), and many are visible on non-contrast MRI.

1.5 Rathke Cleft Cyst

Asymptomatic Rathke cleft cysts are a common incidental finding at autopsy and on MR imaging of the brain. These cysts are predominantly intrasellar in location. In an evaluation of 1000 autopsy specimens, 113 pituitary glands (11.3%) harbored incidental Rathke cleft cysts. Incidental Rathke cysts in a large autopsy series found 89% were localized at the center of the gland, with the remaining 11% predominantly lateral lesions. In that series, of all incidental pituitary lesions localized to the central part of the gland, 87% were Rathke cysts. Extrasellar Rathke cysts typically occur in the suprasellar cistern, usually midline and anterior to the stalk. Rathke cleft cysts are found in all age-groups. They share a common origin with some craniopharyngiomas in that they are thought to originate from remnants of squamous epithelium from the Rathke cleft. The cyst wall is composed of a single cell layer of columnar, cuboidal, or squamous epithelium on a basement membrane. The epithelium is often ciliated and may contain goblet cells. The cyst contents are typically mucoid, less commonly filled with serous fluid or desquamated cellular debris. Calcification in the cyst wall is rare.

Most Rathke cleft cysts are small and asymptomatic. Symptoms occur if the cyst enlarges sufficiently to compress the pituitary gland or optic chiasm and uncommonly, secondary to hemorrhage. The MR signal characteristics vary depending on the cysts contents (protein concentration of mucoid material), with approximately 60% hyperintense on unenhanced T1-weighted images (Fig. 1.2a), and 40% following the signal characteristics of CSF on T1-weighted and T2-weighted images. An “intra-cystic nodule” is diagnostic and is present in up to 75% of cases. These nodules are composed of mucinous material, protein, and cholesterol and are characteristically hypointense on T2-weighted imaging (Fig. 1.2b). The nodules may be hyperintense on T1-weighted imaging and do not enhance. Rathke cleft cysts do not enhance. Occasionally there may be thin marginal enhancement of the cyst wall. This feature can be used to advantage in difficult cases to separate these cysts from craniopharyngiomas.

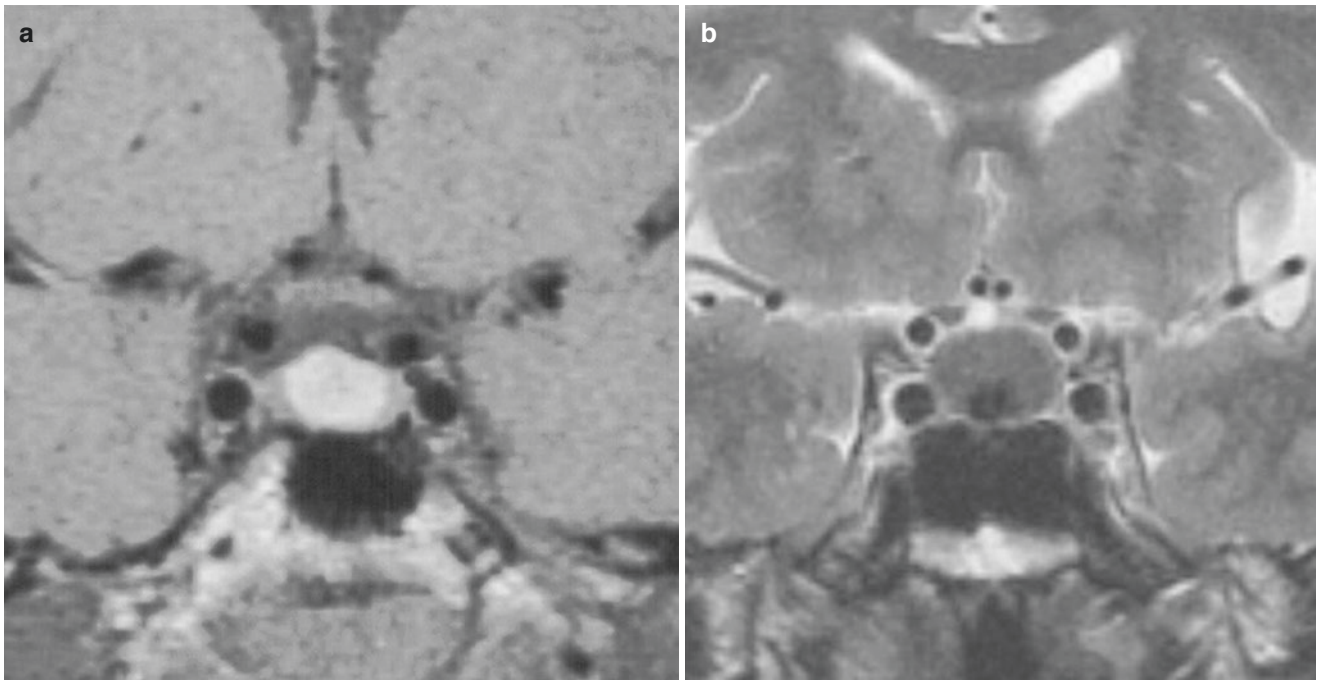


Fig. 1.2 Rathke cleft cyst. Coronal unenhanced T1-weighted MR (a). Coronal T2-weighted MR illustrating a hypointense central “intra-cystic nodule” (b)

1.6 Craniopharyngioma

Craniopharyngiomas are epithelial-derived neoplasms that occur in the region of the sella turcica and suprasellar cistern and less frequently in the third ventricle. Craniopharyngiomas account for approximately 3% of all intracranial tumors and show no gender predominance. Craniopharyngiomas are hormonally inactive lesions, although compression of the stalk may result in diabetes insipidus. They have a bimodal age distribution with more than half occurring in childhood or adolescence, with a peak incidence between 5 and 10 years of age. There is a second smaller peak in adults in the sixth decade of life. These tumors vary greatly in size and most often arise in the suprasellar cistern. Infrequently (5%), craniopharyngiomas are entirely intrasellar.

The most frequent craniopharyngioma is the classic *adamantinomatous* type, identified during the first two decades of life presenting with symptoms and signs of increased intracranial pressure including headache, nausea, vomiting, and papilledema. Visual disturbances due to compression of the optic apparatus are frequent but difficult to detect in young children. Others present with pituitary hypofunction because of compression of the pituitary gland, pituitary stalk, or hypothalamus. Rarely, *adamantinomatous* tumors are found outside the suprasellar cistern, including in the posterior fossa, pineal region, third ventricle, and nasal cavity (sphenoid sinus).

Adamantinomatous tumors are almost always cystic and usually have both solid and cystic components. Calcification is seen in the vast majority (~90%) of these tumors. These calcifications can often be identified on MRI as hypointense foci along the wall of the primary lesion; however, calcifications can be difficult to discern and in such cases CT will prove helpful. Extensive fibrosis and signs of inflammation are often found with these lesions, so that they adhere to adjacent structures including the vasculature at the base of the brain. Optic tract and hypothalamic edema on T2-weighted images is a common associated finding that is not usually seen with pituitary macroadenomas and meningiomas. Due to the inflammatory and fibrotic nature of craniopharyngiomas, recurrence is common, typically within the first 5 years after surgery.

On rare occasions, *adamantinomatous* craniopharyngiomas may be purely solid and completely calcified. These calcified types of tumors can be entirely overlooked on MRI unless close scrutiny is paid to subtle distortion of the normal suprasellar anatomy. Contrast administration shows a moderate degree of enhancement of the solid tumor.

Papillary craniopharyngiomas are typically found in adult patients. These tumors on MR imaging are solid and enhance, without calcification, and may be found within the third ventricle. Although surgery remains the definitive mode of therapy for all craniopharyngiomas, as papillary variants are encapsulated and are readily separable from nearby structures and adjacent brain, they are thought to recur much less frequently than the *adamantinomatous* type.

1.7 Meningioma

Approximately 10% of meningiomas occur in the parasellar region. These tumors arise from a variety of locations around the sella including the tuberculum sellae, planum sphenoidale, clinoid processes, medial sphenoid wing, and cavernous sinus. Meningiomas are usually slow growing and present because of compression on adjacent structures most commonly the pre-chiasmatic optic nerves and optic chiasm resulting in visual symptoms.

Meningiomas are most frequently isointense—and less commonly hypointense—to gray matter on unenhanced T1-weighted sequences. Approximately 50% remain isointense on the T2-weighted sequence, whereas 40% are hyperintense. Meningiomas enhance intensely and homogeneously, often with a trailing edge of thick dura “dural tail sign.” Other diagnostic signs include visualization of a CSF cleft separating the tumor from the brain (and denoting its extra-axial location) and a clear separation of the tumor from the pituitary gland (thus indicating that the tumor is not of pituitary gland origin) (Fig. 1.3). A peripheral black rim occasionally noted at the edges of these meningiomas is thought to be related to surrounding veins. Hyperostosis and calcification are more apparent on CT scan. Vascular encasement is not uncommon, particularly with meningiomas in the cav-

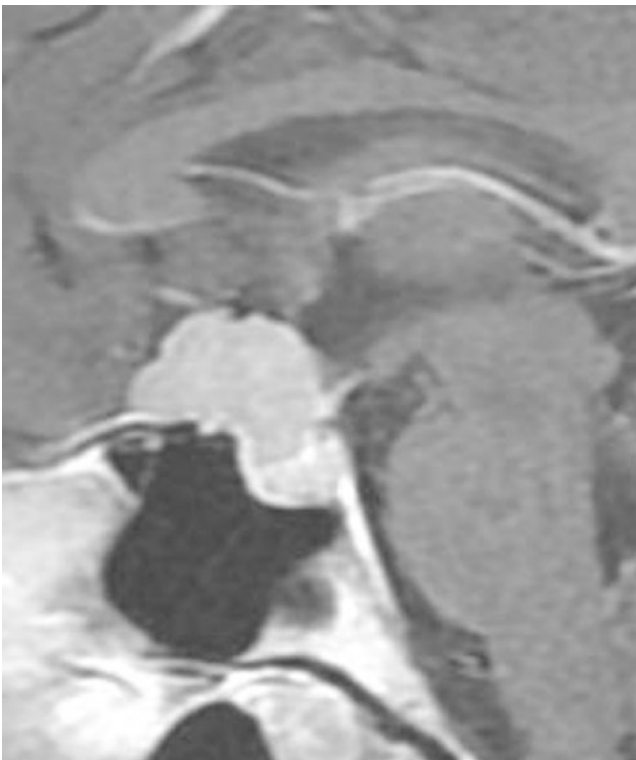


Fig. 1.3 Meningioma. Sagittal contrast-enhanced T1-weighted MR image shows the tumor centered on the planum sphenoidale and tuberculum sellae and illustrates that it is separated from the pituitary gland

ernous sinus. The pattern of encasement is of diagnostic value. Meningiomas typically narrow the lumen of the encased artery (but do not occlude it). This is rare with other tumors most notably pituitary macroadenomas that grow laterally into the cavernous sinus.

1.8 Chiasmatic and Hypothalamic Gliomas

The distinction between chiasmatic and hypothalamic gliomas often depends on the predominant position of the lesion. In many cases, the origin of large gliomas cannot be definitively determined; therefore, hypothalamic and chiasmatic gliomas are discussed as a single entity. The vast majority (75%) of these tumors occur in the first decade of life, with equal prevalence in males and females. There is a definite association of optic nerve and chiasmatic gliomas with neurofibromatosis, more so for tumors that arise from the optic nerve rather than from the chiasm or hypothalamus.

Tumors of chiasmatic origin are also more aggressive than those originating from the optic nerves and tend to invade the hypothalamus and floor of the third ventricle. Patients may experience monocular or binocular visual disturbances, hydrocephalus, or hypothalamic dysfunction. The appearance of the tumor depends on its position and direction of growth. It can be confined to the chiasm or the hypothalamus; however, because of its slow growth, the tumor usually attains a considerable size by the time of presentation, and the site of origin is frequently conjectural. Smaller nerve and chiasmatic tumors are visually distinct from the hypothalamus, and their site of origin is more clear-cut. From the point of view of differential diagnosis, these smaller tumors can be difficult to distinguish from optic neuritis, which can also cause optic nerve enlargement. The clinical history is important in these cases (neuritis is painful, tumor is not) and, if necessary, interval follow-up of neuritis will demonstrate resolution of optic nerve swelling.

On T1-weighted images, these tumors are most often isointense while on T2-weighted images, they are moderately hyperintense. Calcification and hemorrhage are not features of these gliomas but cysts are seen, particularly in the larger hypothalamic tumors. Contrast enhancement occurs in about half of all cases. Because of the tumor's known propensity to invade the brain along the optic radiations, T2-weighted images of the entire brain are necessary. This pattern of tumor extension is readily evident as hyperintensity on the T2-weighted image; however, patients with neurofibromatosis (NF) present a problem in differential diagnosis. This relates to a high incidence of benign cerebral hamartomas and atypical glial cell rests in NF that can exactly mimic glioma. These both appear as areas of high signal intensity on T2-weighted images within the optic radi-

ations. Lack of interval growth and possibly the absence of contrast enhancement are more supportive of a diagnosis of hamartoma while enhancement suggests glioma.

1.9 Metastases

Symptomatic metastases to the pituitary gland are found in 1–5% of cancer patients. These are primarily patients with advanced, disseminated malignancy, particularly breast and lung carcinoma. Intrasellar and juxtaseellar metastases arise via hematogenous seeding to the pituitary gland and stalk, by extension of bone metastases and by CSF seeding. There are no distinctive MRI characteristics of metastases, although infundibular involvement is common, and bone destruction is a prominent feature of lesions that involve the skull base. Metastases involving the sella are not uncommonly misinterpreted as pituitary adenomas. In addition to evaluating the discriminating imaging features, metastases unlike adenomas are often associated with diabetes insipidus.

1.10 Infections

Infection in the suprasellar cistern and cavernous sinuses is usually part of a disseminated process or occurs by means of intracranial extension of an extracranial infection. The basal meninges in and around the suprasellar cistern are susceptible to tuberculous and other forms of granulomatous meningitis. The cistern may also be the site of parasitic cysts, in particular (racemose and subarachnoid) neurocysticercosis. In infections of the cavernous sinus, many of which are accompanied by thrombophlebitis, the imaging findings on CT and MRI consist of a convex lateral contour to the affected cavernous sinus with evidence of a filling defect after contrast administration. The intra-cavernous portion of the internal carotid artery may also be narrowed secondary to surrounding inflammatory change.

Infections of the pituitary gland itself are uncommon. Direct viral infection of the hypophysis has never been established, and bacterial infections are unusual. There has been speculation that cases of acquired diabetes insipidus may be the result of a select viral infection of the hypothalamic supra-optic and paraventricular nuclei. Tuberculosis and syphilis, previously encountered in this region because of the higher general prevalence of these diseases in the population, are now uncommon. Gram-positive cocci are the most frequently identified organisms in pituitary abscesses. Pituitary abscesses usually occur in the presence of other sellar masses such as adenomas, Rathke's cleft cysts, and craniopharyngiomas, indicating that these masses serve as predisposing factors to infection.

There are a few reports on CT of pituitary abscesses. These indicate that the lesion is similar in appearance to an adenoma. The correct preoperative diagnosis of abscess is difficult and rarely made. Non-contrast MRI demonstrates a sellar mass indistinguishable from an adenoma. Occasionally, pituitary abscesses are unrelated to primary pituitary lesions. In these cases, erosion of the bony sella from an aggressive sphenoid sinusitis may be the route of infection.

1.11 Noninfectious Inflammatory Lesions

Lymphocytic hypophysitis is an uncommon, noninfectious inflammatory disorder of the pituitary gland. It occurs almost exclusively in women and particularly during late pregnancy or in the post-partum period. The diagnosis should be considered in a peripartum patient with a pituitary mass, particularly when the degree of hypopituitarism is greater than that expected from the size of the mass. It is believed that, if untreated, the disease results in panhypopituitarism. Clinically, the patient complains of headache, visual loss, inability to lactate, or some combination thereof. Pituitary hormone levels are depressed. MRI shows diffuse enlargement of the anterior lobe without focal abnormality or change in internal characteristics of the gland. Thickening of the pituitary stalk may also be present.

Sarcoid afflicting the hypothalamic–pituitary axis usually manifests itself clinically as diabetes insipidus, or occasionally as a deficiency of one or more anterior lobe hormones. Low signal intensity on T2-weighted images is one finding that occurs in sarcoid with some frequency, but rarely in other diseases, with few exceptions (other granulomatous inflammatory diseases, lymphoma, some meningiomas). This low signal finding may aid in differential diagnosis. Also, the presence of multiple, scattered intra-parenchymal brain lesions should raise the possibility of the diagnosis, as should diffuse or multifocal lesions of the basal meninges. The latter are best defined on coronal contrast-enhanced T1-weighted images.

Tolosa-Hunt syndrome (THS) refers to a painful ophthalmoplegia caused by an inflammatory lesion of the cavernous sinus that is responsive to steroid therapy. Pathologically, the process is similar to orbital pseudotumor. Imaging in this disorder is often normal or may show subtle findings such as asymmetric enlargement of the cavernous sinus, enhancement of the prepontine cistern, or abnormal soft tissue density in the orbital apex. Hypointensity on T2-weighted images may be observed; since this observation is uncommon in all but a few other diseases (e.g., meningioma, lymphoma, and sarcoid), it may be helpful in the diagnosis. Clinical history allows further precision in differential diagnosis—meningioma does not respond to steroids while lymphoma and sarcoid have evidence of disease elsewhere in almost all cases.

1.12 Vascular Lesions

Saccular aneurysms in the sella turcica and parasellar area arise from either the cavernous or supra-clinoid segments of the internal carotid artery. It is extremely important to identify these lesions. Confusion with a solid tumor can lead to surgical catastrophes. Fortunately, their MRI appearance is distinctive. Aneurysms are well defined and lack internal signal on spin echo (SE) images, the so-called signal void created by rapidly flowing blood. This blood flow may cause artifacts on the image usually manifest as multiple ghosts in the phase-encoding direction, and in itself is a useful diagnostic sign.

Thrombus in the aneurysm lumen fundamentally alters these characteristics, the clot usually appearing multi-lamellated high signal on T1-weighted images, partially or completely filling the lumen. Hemosiderin from superficial siderosis may be visible in the adjacent brain manifest as low signal intensity on T2-weighted, gradient echo, or susceptibility-weighted images. MR or CT angiography is used to confirm the diagnosis, define the neck of the aneurysm, and establish the relationship of the aneurysm to the major vessels.

Carotid cavernous fistulas are abnormal communications between the carotid artery and the cavernous sinus. Most cases are due to trauma; less frequently they are “spontaneous.” These spontaneous cases are due to a variety of abnormalities, including atherosclerotic degeneration of the arterial wall, congenital defects in the media, or rupture of an internal carotid aneurysm within the cavernous sinus. Dural arteriovenous malformations (AVMs) of the cavernous sinus are another form of abnormal arteriovenous (AV) communication in this region.

On MRI, the dilatation of the venous structures, in particular the ophthalmic vein and cavernous sinus, is usually clearly visible. The inter-cavernous venous channels dilate in both direct and indirect carotid cavernous fistulae and may also be seen on MR images. Furthermore, the internal character of the cavernous sinus is altered; definite flow channels become evident secondary to the arterial rates of flow within the sinus. The fistulous communication itself is most often occult on MRI. The pituitary gland has been noted to be prominent in cases of dural arteriovenous fistula without evidence of endocrine dysfunction. The exact mechanism of pituitary enlargement is not known, however venous congestion is a postulated cause.

Cavernous hemangiomas are acquired lesions and not true malformations and rarely may occur in the suprasellar cistern. They may have an atypical imaging appearance so some caution must be exercised in the differential diagnosis of parasellar masses. Even though cavernous hemangiomas in this location are rare, failure of the surgeon to appreciate

their vascular nature can lead to unanticipated hemorrhage. Cavernous hemangiomas should be considered in the differential diagnosis of solid, suprasellar masses that do not have the classic features of more common lesions, in particular craniopharyngiomas or meningiomas. On MR imaging, T2-weighted images are helpful as hemangiomas are often markedly T2 hyperintense compared to meningiomas, and hemangiomas may have a peripheral dark rim.

Other vascular abnormalities of the sella include unilateral tortuous or bilateral “kissing” internal carotid arteries and medial trigeminal artery. While the former are relatively straightforward on imaging, the medial trigeminal artery is worth remembering. Much like with the intrasellar aneurysm, with the medial trigeminal artery, neurosurgical catastrophes can occur if the presence of an intrasellar artery is not identified. This artery will arise from the medial aspect of the cavernous carotid artery and will course directly posteriorly through the gland and through the dorsum sellae to reach the basilar artery. Approximately 40% of trigeminal arteries arise medially. In addition, patients with trigeminal arteries are at increased risk of associated intracranial aneurysm. Finally, congenital absence of the internal carotid artery and asymmetric pneumatization of the sphenoid and sella can pose confusing images.

Key Points

- Carotid artery aneurysms and anomalies can mimic intrasellar and parasellar mass lesions. Arterial lesions must be considered in the differential diagnosis of lesions in this area. MRA or CTA can be used to confidently confirm or exclude the presence of arterial lesions.

1.13 Additional Pathology in the Sellar and Parasellar Regions

Many other lesions may involve the sella turcica and parasellar region. These include mass lesions such as germinoma, epidermoid, dermoid, teratoma, schwannoma, chordoma, ecchordosis, choristoma, arachnoid cyst, hamartoma, IgG4-related disease, and Langerhans cell histiocytosis. Also, there are several important metabolic conditions that may cause pituitary dysfunction or MRI-observable abnormalities in and around the sella. These include diabetes insipidus, growth hormone deficiency, hemochromatosis, hypermagnesemia, and hypothyroidism. Space limitations preclude their further discussion in this synopsis.

1.14 Concluding Remarks

An understanding of the physiology of the pituitary gland and stalk, as well as the anatomy of the sella turcica and surrounding structures is important. There are 3 or 4 common pathologies that arise from each of these regions (sella turcica, suprasellar cistern, cavernous sinus). Knowledge of the anatomy, physiology, and familiarity with these pathologies results in high probability of correct imaging diagnosis.

Take-Home Messages

- The vast majority of lesions arising in the sella turcica are pituitary adenomas.
- You do not want to miss aneurysms and arterial anomalies.
- Anatomic relationships are key to arriving at a correct imaging diagnosis.
- Knowledge of basic physiology and clinical presentation helps synch the diagnosis.

Further Reading

Araujo-Castro M, Acitores Cancela A, Vior C, Pascual-Corrales E, Rodríguez Berrocal V. Radiological Knosp, revised-Knosp, and Hardy–Wilson classifications for the prediction of surgical outcomes in the endoscopic endonasal surgery of pituitary adenomas: study of 228 cases. *Front Oncol.* 2022;11:807040.

Byun WM, Kim OL, Kim D. MR imaging findings of Rathke’s cleft cysts: significance of intracystic nodules. *AJNR Am J Neuroradiol.* 2000;21(3):485–8.

Chapman PR, Singhal A, Gaddamanugu S, Prattipati V. Neuroimaging of the pituitary gland: practical anatomy and pathology. *Radiol Clin N Am.* 2020;58(6):1115–33.

Chatain GP, Patronas N, Smirniotopoulos JG, Piazza M, Benzo S, Ray-Chaudhury A, Sharma S, Lodish M, Nieman L, Stratakis CA, Chittiboina P. *J Neurosurg.* 2018;129(3):620–8.

Kucharczyk W, Peck WW, Kelly WM, Norman D, Newton TH. Rathke cleft cysts: CT, MR imaging and pathologic features. *Radiology.* 1987;165:491–5.

Langlois F, Varlamov EV, Fleseriu M. Hypophysitis, the growing spectrum of a rare pituitary disease. *J Clin Endocrinol Metab.* 2022;107(1):10–28.

Lundin P, Bergström K, Nyman R, Lundberg PO, Muhr C. Macroprolactinomas: serial MR imaging in long term bromocriptine therapy. *AJNR Am J Neuroradiol.* 1992;13:1279–91.

Manara R, Maffei P, Citton V, et al. Increased rate of intracranial saccular aneurysms in acromegaly: an MR angiography study and review of the literature. *J Clin Endocrinol Metab.* 2011;96(5):1292–757.

Nagahata M, Hosoya T, Kayama T, Yamaguchi K. Edema along the optic tract: a useful MR finding for the diagnosis of craniopharyngiomas. *AJNR Am J Neuroradiol.* 1998;19:1753–7.

Naylor MF, Scheithauer BW, Forbes GS, Tomlinson FH, Young WF. Rathke cleft cyst: CT, MR, and pathology of 23 cases. *J Comput Assist Tomogr.* 1995;19(6):853–9.

Oka H, Kawano N, Suwa T, Yada K, Kan S, Kameya T. Radiological study of symptomatic Rathke’s cleft cysts. *Neurosurgery.* 1994;35(4):632–6.

Pinker K, Ba-Ssalamah A, Wolfsberger S, Mlynarik V, Knosp E, Trattig S. The value of high-field MRI (3T) in the assessment of sellar lesions. *Eur J Radiol.* 2005;54(3):327–34.

Steiner E, Knosp E, Herold CJ, et al. Pituitary adenomas: findings of postoperative MR imaging. *Radiology.* 1992;185:521–7.

Teramoto A, Hirakawa K, Sanno N, Osamura Y. Incidental pituitary lesions in 1000 unselected autopsy specimens. *Radiology.* 1994;193:161–4.

Wolfsberger S, Ba-Ssalamah A, Pinker K, Mlynarik V, Czech T, Knosp E, Trattig S. Application of three-tesla magnetic resonance imaging for diagnosis and surgery of sellar lesions. *J Neurosurg.* 2004;100(2):278–86.

Open Access This chapter is licensed under the terms of the Creative Commons Attribution 4.0 International License (<http://creativecommons.org/licenses/by/4.0/>), which permits use, sharing, adaptation, distribution and reproduction in any medium or format, as long as you give appropriate credit to the original author(s) and the source, provide a link to the Creative Commons license and indicate if changes were made.

The images or other third party material in this chapter are included in the chapter's Creative Commons license, unless indicated otherwise in a credit line to the material. If material is not included in the chapter's Creative Commons license and your intended use is not permitted by statutory regulation or exceeds the permitted use, you will need to obtain permission directly from the copyright holder.

